Oligomerization of Light−Harvesting I Antenna Peptides of Rhodospirillum rubrum †

ARTICLE *in* BIOCHEMISTRY · NOVEMBER 2001

Impact Factor: 3.02 · DOI: 10.1021/bi010163f · Source: PubMed

Oligomerization of Light-Harvesting I Antenna Peptides of *Rhodospirillum rubrum*†

Anjali Pandit,*,‡ Ronald W. Visschers,§ Ivo H. M. van Stokkum,|| Ruud Kraayenhof,‡ and Rienk van Grondelle||

Department of Structural Biology, Faculty of Biology Vrije Universiteit Amsterdam, De Boelelaan 1087, 1081 HV Amsterdam, The Netherlands, Division of Physics and Astronomy, Faculty of Sciences, Vrije Universiteit Amsterdam, De Boelelaan 1087, 1081 HV Amsterdam, The Netherlands, and NIZO Food Research, Kernhemseweg 2, 6710 BA Ede The Netherlands

Received January 25, 2001; Revised Manuscript Received July 19, 2001

ABSTRACT: We investigated the oligomerization of the core light-harvesting complex (LH1) of *Rhodospirillum rubrum* from the separated $\alpha\beta$ $BChl_2$ subunits (B820) and the oligomerization of the B820 subunit from its monomeric peptides. The full LH1 complex was reversibly associated from B820 subunits by either varying the temperature in the range 277−300 K or by varying the detergent concentration in the buffer from 0.36 to 0.52% *n*-octyl-β-D-glucopyranoside. Temperature-induced transition measurements showed hysteresis: raising the temperature induced dissociation of B873 directly into B820 subunits whereas upon recooling an intermediate spectral form was observed with an absorption maximum located around 850 nm. This intermediate form was also observed in detergent-induced transitions. It is speculated that the B850 form is a small aggregate of B820, for instance a dimer. Additionally, during a temperature-mediated transition at low detergent concentration, a set of spectral forms with maxima slightly blue-shifted from 873 nm were observed, possibly due to opened rings with one or only a few $\alpha\beta$ $BChl_2$ units missing. The temperature-induced transition of LH1 is discussed in terms of a simple assembly model. It is concluded that a moderately cooperative assembly explains the formation of small aggregates of B820 as well as of incomplete rings. Furthermore, the B820 subunits were reversibly dissociated into the monomeric B777 form by increasing either the temperature or the detergent concentration. Estimations of the enthalpy and entropy changes for the dimeric association reaction of B777 into B820 yielded an enthalpy change of -216 kJ mol^{-1} and an entropy change of -0.59 kJ $mol^{-1}K^{-1}$, at a detergent concentration of 0.8% *n*-octyl-β-D-glucopyranoside.

The light-harvesting complexes in the membranes of photosynthetic bacteria are responsible for the initial capture of light and transfer of excitation energy to the photosynthetic reaction centers. In purple non-sulfur bacteria, two types of light-harvesting complexes occur: the LH1[1] core antenna surrounding the reaction center and the LH2 peripheral antenna that is connected to the LH1 (*1*−*4*). Both types of complexes consist of ringlike oligomers of two types of pigment−protein subunits, the so-called α and β polypeptides, that each bind one or two bacteriochlorophyll pigments. For all species, both the α and β polypeptide contain one transmembrane α-helical stretch as a highly conserved structural element (*1*, *5*). The structures of LH2 of *Rhodopseudomonas. acidophila* (*6*) and LH2 of *Rhodospirillum. molischianum* (*7*) have been resolved to high resolution: both complexes were shown to contain an inner ring of α-polypeptides and an outer ring of β-polypeptides with a ring of bacteriochlorophylls, absorbing at 850 nm and called B850s, sandwiched between the two rings. Between the β-polypeptides, a second ring of bacteriochlorophylls absorbing at 800 nm occurs, and these are called B800s and are positioned parallel to the membrane plane, close to the cytosolic surface. The LH2 ring of *Rps. acidophila* has a C_9 symmetry and contains 18 B850 and 9 B800 bacteriochlorophylls. The LH2 ring of *Rs. molischianum* has a C_8 symmetry. For LH1, only a low resolution structure exists that shows many similarities to those of LH2 but has C_{16} symmetry (*8*). In vivo, these complexes may occur in the form of stacked dimers of RC-LH1 (*9*, *10*, *11*) in which the ring is only occupied for three-quarters.

The LH1 complexes of the purple bacteria *Rs. rubrum*, *Rps. marina*, *Rps. viridis*, and *Rb. sphaeroides* can be dissociated into subunits absorbing at 820 nm, called B820, by treatment with detergent and extraction of the carotenoids. These subunits are the building blocks of the oligomeric LH1 complexes and consist of an $\alpha\beta$ heterodimer and two bacteriochlorophylls. Exciton coupling between the two bacteriochlorophyll molecules of the B820 subunit is probably the cause of the red-shift from 770 to 777 nm toward 820 nm. For *Rs. rubrum* a mutant strain, called G9+, exists that produces LH1 complexes lacking carotenoids. Isolated LH1 antenna complexes of this strain can be reversibly dissociated into B820 subunit pigment−protein complexes (*12*−*14*), which can be further dissociated into monomeric

† This work was financially supported by The Netherlands Organization of Scientific Research (NWO) via the Foundation of Earth and Life Sciences (ALW).

* To whom correspondence should be addressed. Fax: +31-20-4447157. Phone: +31-20-4447166. E-mail pandit@bio.vu.nl.

‡ Department of Structural Biology.

§ NIZO Food Research.

|| Division of Physics and Astronomy.

[1] Abbreviations: BChl, bacteriochlorophyll; LH1, the core light-harvesting complex; LH2, the peripheral light-harvesting complex; RC, reaction center; OG, *n*-octyl-β-D-glucopyranoside; CMC, critical micelle concentration; fwhm, full-width half-maximum.

10.1021/bi010163f CCC: $20.00
Published on Web 10/02/2001

polypeptides, called B777 and absorbing at 777 nm (*15*). Both the B820 subunit and the LH1 complex have also been reconstituted from the separately isolated components (*16*−*18*). The isolated B820 subunit of this mutant strain is believed to be composed either of one αβ-polypeptide pair and two BChl molecules (*13*, *19*) or of two αβpolypeptide pairs and four BChl molecules (*14*, *15*). However, spectroscopic evidence strongly favors B820 being a dimer of bacteriochlorophylls (*20*−*22*).

Several studies have investigated what stabilizes the assembly of bacterial light-harvesting complexes. First, bacteriochlorophyll pigments contribute to the stabilization of both the full complexes and the dimeric subunits. It has been shown that dimerization of free BChl *a* pigments in a formamide/water solution gives a change in Gibbs free energy of −9.2 kcal mol^{-1} (*23*). The central Mg atom in the bacteriochlorophyll rings is a structural requirement for BChl binding to form the subunit complex and LH1 of *Rs. rubrum* and *Rb. sphaeroides* (*17*). It coordinates to a highly conserved histidine imidazole group located in the transmembrane section of the polypeptides (*24*), with a binding energy due to ligand formation estimated to be approximately 5 kcal mol^{-1} per BChl (*25*). The C13^2 carbomethoxy and the C_9 keto carbonyl group of the BChl *a* contribute to the stability of the heterodimer. It is proposed that the α-bound BChl is hydrogen bonded to the His residue of the β-polypeptide and vice versa (*26*). For stability of the full LH1 complex, the C3^1 carbonyl group is important. For each subunit this group is hydrogen bonding with the Trp11 residue of the α-polypeptides of the preceding subunit (*17*, *27*−*29*). The latter group is required for LH1 formation of both *Rs. rubrum* and *Rb. sphaeroides*, but not for subunit formation of *Rs. rubrum* (*19*). Second, ion pairing of amino acid residues contributes to stabilization of both the dimer subunits and the full complex. Experiments on truncated polypeptides and from site-directed mutagenesis experiments reveal that at least one ion pair contributes to stabilization of the dimer, with a binding energy of approximately 3 kcal mol^{-1} (*19*). This ion pairing is suggested to involve the Asp-20 of the α-polypeptides and the His-18 of the β-polypeptides. Two other ion pairs may occur between groups in the N-terminal region of the α- and β-polypeptides, corresponding to pairs of strictly conserved amino acids. Third, carotenoids are important for stabilization of the LH1 ring. They need to be removed to induce dissociation of the ring complexes into subunits and facilitate reconstitution of LH1 from the separated subunits (*17*). The increase of stability of the complex in the presence of carotenoids is presumed to stem from packing between the rigid conjugated double bond chain of the carotenoid molecules with its periodically protruding methyl groups and the αβ2BChl units (*19*). Fourth, both the subunits and the full complex are stabilized by packing of the hydrophobic amino acid residues (*19*). Sturgis and Robert concluded that the major enthalpy change for association of B777 monomers into B820 subunits has to be caused by burying of the hydrophobic regions (*15*).

On the basis of sequence alignment, modeling, and spectroscopic studies, similarities are expected between the binding sites of the B850 ring of LH2 and the core LH1 (*30*, *26*). Comparison of site-directed modification of the ligands to the BChls of LH1 and LH2 complexes of *Rb. sphaeroides* revealed that for both LH1 and LH2 the His-residue is necessary for correct assembly: mutation of the His-residue of the α or β polypeptides of LH1 and LH2 resulted in the absence of LH1 and LH2 complexes or unstable LH1 complexes (*26*). Nevertheless, major differences between the LH1 and LH2 complexes must exist with respect to their structure and stability, since no LH1 complexes have been crystallized and no carotenoidless mutants of LH2 exist.

The functioning of the above-mentioned membrane proteins largely depends on correct folding and assembly; however, the driving force for this assembly is not fully understood. Few studies have investigated the thermodynamic parameters that induce folding and assembly of transmembrane proteins. In contrast to water-soluble proteins, the folding of membrane proteins can usually not be induced or modulated in vitro and a membrane environment has to be introduced. This complicates studying the energetics and kinetics of the assembly of these proteins. Therefore, the isolated LH1 antenna complex of the *Rs. rubrum* G9 strain forms a suitable system for study of protein assembly. Dissociation of the protein into subunits or into monomeric polypeptides and reconstitution into the full complex can be modulated by varying the type and concentration of detergent used for solubilization, by varying the temperature, or by varying the protein concentration. The strong red shift of the Q_y absorption band upon association of the monomeric polypeptides into subunits and further red shift upon assembly to the complete LH1 ring provides a spectroscopic tool to measure the oligomeric state of the protein. The thermodynamics for the association of monomeric polypeptides of the G9 mutant of *Rs. rubrum* into B820 subunits have been investigated (*15*) as well as the stability of the monomeric peptides, the separated subunits, and the LH1 complex (*31*). Up to date, only little information is available about the thermodynamics for the assembly of the full complex.

In this work, we have investigated the full oligomerization of the LH1 ring complex from B820 subunits and the oligomerization of the B820 subunit from the B777 monomers. Our work is an extension of the studies of Miller et al. (*13*) and van Mourik et al. (*32*) and aims to further characterize the physical and chemical parameters that control the oligomerization of this membrane complex. Samples were prepared in buffer containing octylglucoside (OG), based on earlier studies that have shown that carotenoidless B873 complexes of *Rs. rubrum* dissolved in this detergent can reversibly be dissociated into its B820 subunits (*13*, *32*), whereas after treatment with other detergents dissociation directly into B777 monomers was observed (*13*, *14*). We used the fact that the reversible dissociation of B873 into B820 subunits can be obtained not only by treatment with detergent, but also by varying the temperature in the range 278−300 K. This temperature dependence was observed already by Miller et al. (*13*). The latter finding provided us with a controlable method to modulate the reversible association reaction without changing sample. Because in our temperature experiments the suitable temperature range was limited from 273 K to about 313 K (above 313 K the bacteriochlorophyll pigments dissociate from the peptides), the detergent concentration had to be in the range 0.5−0.8% OG to modulate the full association or dissociation reaction. It is unclear at which precise detergent concentration OG

reaches it critcal micelle concentration (CMC). Therefore, we performed temperature-mediated association experiments using two sample preparations containing either 0.54 or 0.8% OG that should reflect two different conditions in terms of micellization. In addition to our temperature experiments, dissociation of B873 into B820 subunits was induced by increasing the detergent concentration from 0.36 to 0.52%, in samples measured at room temperature. We present the observation of an intermediate spectral form appearing in the reassociation from B820 subunits to the full B873 complex, strongly suggesting that the assembly of the LH1 ring occurs via intermediate oligomeric states. Further, the reversible dissociation of B820 into B777 was studied by conducting experiments in which either the temperature, the detergent concentration, or the protein concentration was varied. From these experiments, the stoichiometry and the entropic and enthalpic contributions to the free energy of the B777−B820 transition have been determined.

1. MATERIALS AND METHODS

n-Octyl-β-D-glucopyranoside (OG) was obtained from Calbiochem (San Diego, CA). The purified B820(OG) complexes were prepared from the carotenoidless strain *Rs. rubrum* G9. Cells were grown at 400 lux and 20 °C and harvested by two cycles of centrifugation (15 min at 4 °C at 7500*g*) and washing with 10 mM Hepes, pH 8. Chromatophores were prepared by sonication followed by centrifugation and subsequently purified by sucrose density centrifugation, centrifugating one night at 4 °C and at 37000*g*, using a sucrose gradient of 45% sucrose, 40% sucrose, and 5% sucrose (g/g). Purified chromatophores were stored in the sucrose medium at −70 °C until further use. For preparation of the B820(OG) subunits, chromatophores were diluted with 50 mM potassium phosphate buffer pH 8 to an OD_{875} of 3 (60 mL). OG was added to it (0.6 g) and the suspension was centrifuged with 37000*g* at 10 °C for removal of unsolubilized material and concentrated by pressing through a filter (Amicon, YM10). Badges of 200 mL were applied to a Superose-6 FPLC column (Pharmacia, Uppsala, Sweden) that was equilibrated with 50 mM potassium phosphate buffer and 0.5% OG. The column was eluted at 0.4 mL/min and the OD_{820} peak was collected. The collected B820(OG) was stored at −80 °C until use. All preparations were carried out in dimmed light to prevent degradation of the BChl *a*.

Samples were prepared by diluting stock solutions in buffer containing 50 mM potassium phosphate, pH 7.5, and 0.8% OG unless stated otherwise. The concentration BChl in each sample was determined by measuring the absorption at 770 nm of a small amount diluted in diethyl ether, using the extinction coefficient $\epsilon_{770} = 95\ mM^{-1}\ cm^{-1}$ (*34*). Absorption spectra were measured on a Perkin-Elmer Lambda 40 UV−Vis Spectrofotometer using a resolution of 4 nm.

Global analysis fitting of the spectra measured as a function of temperature or detergent concentration was performed using a spectral model (*35*) and constraints on some of the amplitudes. Other fitting of data was performed using a least-squares fitting procedure and programmed in Igor Pro (WaveMetric Inc.). Calculation of the kinetic assembly models was performed using Mathcad Plus 5.0 (MathSoft Inc., Massachusetts).

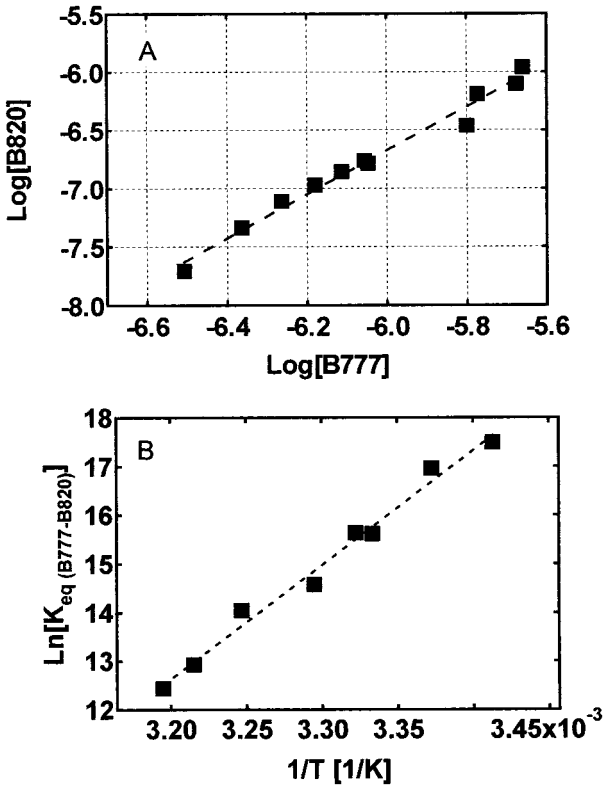

FIGURE 1: Logarithm of the concentration B820 subunits plotted versus the logarithm of the concentration B777 (A) and a Hill plot for the B777−B820 association (B). (A) To obtain the data plotted here, a series of absorption spectra with increased protein concentration was fitted with a linear combination of a B820 and a B777 spectrum to estimate the concentration of each species. The detergent concentration was 0.8% OG. A linear fit (dashed line) yields a slope of 1.88 (0.08), giving the stoichiometric number for the association reaction of B777 into B820 subunits. (B) The linear logarithm of the association constants for the association of B777 into B820 are plotted versus the reciprocal temperature. The change in free enthalpy $\Delta H°$ is −216 (30) kJ mol^{-1} and the change in free entropy is $\Delta S°$ is −0.59 (0.10) kJ $mol^{-1}K^{-1}$. To obtain the association constants, a series of absorption spectra with increased temperature was fitted with a linear combination of a B820 and a B777 spectrum to estimate the concentration of each species. Assuming a dimeric association reaction, the association constants were calculated from $K_a = [B820]/[B777]^2$.

2. RESULTS

2.1. Oligomerization of B777 into B820. Association of the B777 monomers to B820 units was achieved by either (1) increasing the concentration of protein (raising the concentration from 0.1 μM of BChl to 0.25 μM, assuming that all BChl was bound to the polypeptides) at room temperature, or (2) lowering the temperature from 312 to 281 K or (3) lowering the detergent concentration from 1.2 to 0.4%. In the first two cases, the detergent concentration was 0.8%. In all cases, the absorption spectra show a shift from 777 nm toward 820 nm with a well-defined isosbestic point around 795 nm. This indicated the absence of intermediate conformations. The fractions of B777 and B820 in each sample were estimated by fitting of the spectra with a linear combination of a B777 and a B820 spectrum. Figure 1A shows data obtained from absorption spectra of a range of samples with different protein concentrations. For each sample, the logarithm of the concentration of B820 is plotted versus the logaritm of the concentration of B777. A slope

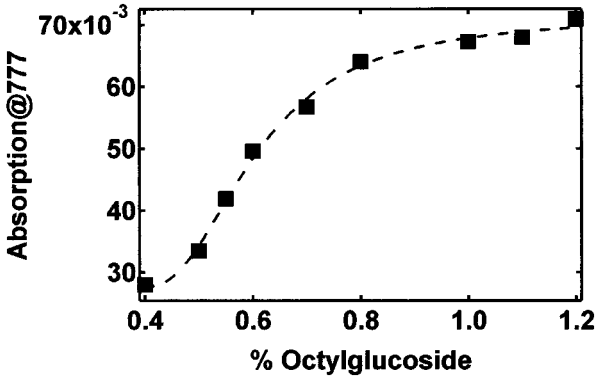

FIGURE 2: Dissociation of B820 into B777 induced by OG. A sigmoidal fit yields a midpoint of 0.61%. This conforms to an addition of 0.21% OG to the concentration of 0.4%, present at the onset of dissociation of B820 into B777, for half-dissociation.

of $n = 1.88$ (0.08) indicates that in the association reaction two B777 monomers associate to form one B820 dimer. This agrees with the studies of Miller et al. who found a stoichiometry of two for the BChl to α and β polypeptides (*13*). For calculation of the association constants, we assumed that such a dimerization reaction is indeed leading to the formation of B820. Figure 1B shows data obtained from absorption spectra of one sample thermostated at different temperatures. In a Hill plot, the linear logarithm of the association constants are plotted versus the reciprocal temperature to estimate the relative enthalpy and entropy contributions to the change in the Gibbs free energy. From the plot, the change in enthalpy $\Delta H°$ was estimated to be -216 (30) kJ mol^{-1} and the change in entropy $\Delta S°$ to be -0.59 (0.10) kJ mol^{-1} K^{-1}. Figure 2 shows the dissociation of B820 into B777 monomers as a function of the detergent concentration. Note that the B820 preparation already contains 0.4% OG. Apparently the further addition of 0.21% OG at the onset of dissociation resulted in half-dissociation of the B820 subunits. This conforms to further addition of about 16 000 OG molecules/B777 monomer. No reaction stoichiometry can be calculated from this, because the fraction of the added detergent that self-aggregates to form micelles is unknown.

2.2. Oligomerization of B820 into B873. Transition between the B873 complex and the B820 subunits was modulated in two ways: in the first the detergent concentration was varied from 0.37 to 0.52% using samples with a fixed protein concentration and measured at room temperature. In the second, a sample was thermostated at temperatures ranging from 280 to 300 K. Figure 3 shows absorption spectra of samples containing different detergent concentrations. Clearly, the shift from B873 to B820 can be observed. However, the spectra did not show an isosbestic point and could not be fitted with a linear combination of a B820 spectrum and a B873 spectrum. This indicates the existence of other spectral forms than the B820 and B873 (see below). In Figure 4, the absorption at 872 nm is plotted versus the concentration of detergent (OG). Apparently, the further addition of 0.0387% OG at the onset of dissociation resulted in half-dissociation of B873 into B820 and/or the intermediate form(s). This conforms to further addition of about 1100 OG molecules per α or β monomer. The detergent-dependent dissociation curve for dissociation of B873 into B820 (Figure 5) is much steeper than the dissociation curve for dissociation

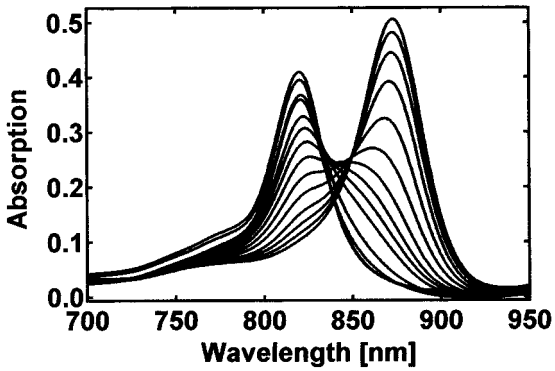

FIGURE 3: Detergent-induced dissociation of B873 into B820 subunits. The concentration OG was raised from 0.376 to 0.520% (higher concentrations OG corresponding to an increase at 820 nm).

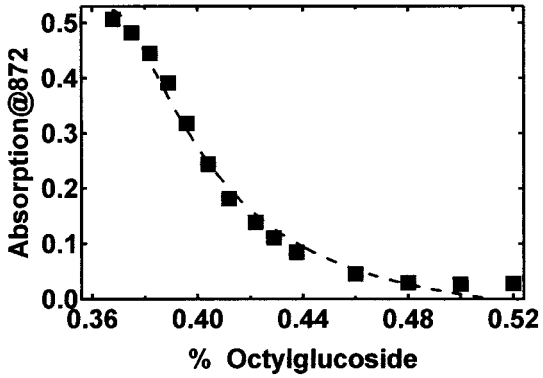

FIGURE 4: The dissociation of B873 into B820 induced by OG. A sigmoidal fit yields a midpoint of 0.407%. This conforms to an addition of 0.0387% OG to the concentration present on the onset of the dissociation for half-dissociation.

of B820 into B777 (Figure 3), indicating a stronger reaction of the detergent molecules with B873 complexes than with B820s and probably reflecting cooperative interactions between B820 subunits to form B873.

Figure 5, panels A and B, show the temperature-induced dissociation and reassociation of B873 in B820, respectively. After each temperature step and thermostating, spectra of the sample at the new temperature were recorded with intervals of 15 min. If no change was observed in this time span, the sample was considered to be in equilibrium. For heating of the sample, this usually was the case within 15 min. For recooling, this could take about 45 min. The dissociation process was completely reversible and the full B873 complex could be reassociated again from the B820 subunit form by lowering the temperature. However, absorption spectra from heated samples at half-dissociation did not at all resemble absorption spectra from recooled samples taken at the same temperatures during the reassociation process. This "hysteresis" effect was reproducible and was observed in all measurements where samples were heated and recooled again. In Figure 5A, the spectra are shown of a sample that was subsequently heated from 280 to 300 K in nine steps, with the spectra taken at the successive temperature intervals (spectra with increased absorption at 820 nm correspond to higher temperatures). The spectra of heated samples exhibited all the features for a two-state dissociation reaction with a clear isosbestic point located at 833 nm. In contrast to this, spectra of recooled samples did not have a clear isosbestic point. Figure 5B shows the same

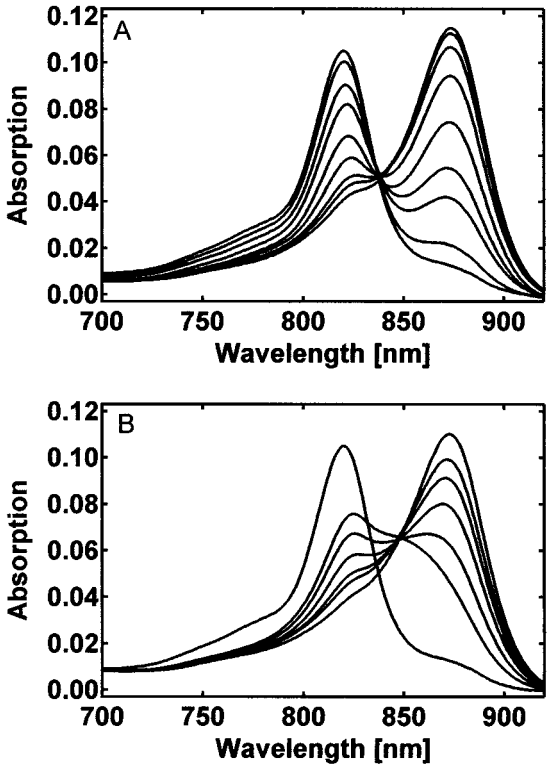

FIGURE 5: Temperature-induced dissociation of B873 into B820 subunits (A) and reassociation of B820 into B873 (B) in the presence of 0.8% OG, showing hysteresis. The temperature was raised from 282 to 300 K in equal steps (A, higher temperatures corresponding to a disappearing peak at 873 nm) and lowered again to 282 K (B, lower temperatures corresponding to an increased peak at 873 nm). All spectra shown are taken from one sample, prepared in 0.8% OG.

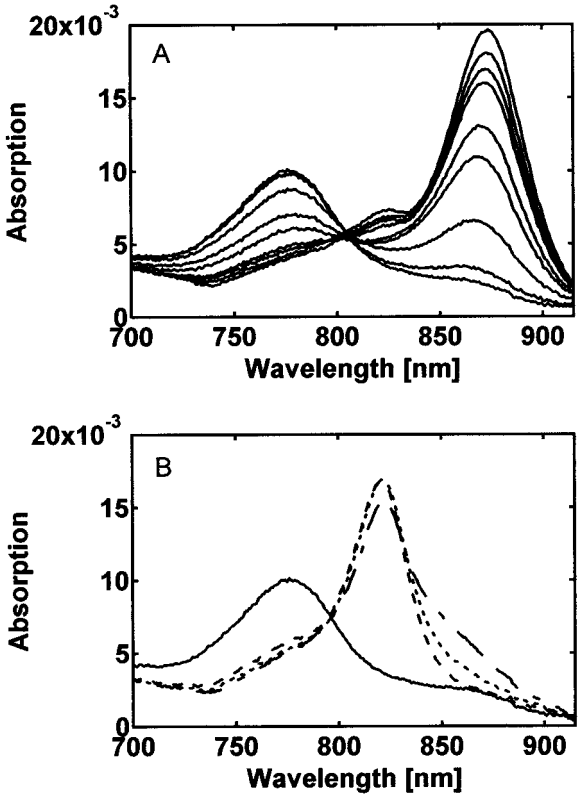

FIGURE 6: Temperature-induced dissociation of B873 into B777 (A) and reassociation into B820 (B) in the presence of 0.54% OG. The temperature was raised from 283 to 302 K in equal steps (A, higher temperatures corresponding to a disappearing peak at 873 nm) and lowered again to 282 K (B, straight line $T = 302$ K, dashed line $T = 286$ K, dotted line $T = 284$ K and dashed−dot line $T = 282$ K). All spectra shown are taken from one sample, prepared in 0.54% OG.

sample, recooled again to 280 K with spectra taken at different temperature intervals (spectra at lower temperatures corresponding to decreased absorption at 820 nm). In fact, the spectra measured in this manner were very similar to spectra obtained in the detergent-variation experiment and could also not be fit by taking a linear combination of a B820 and a B873 spectrum.

Temperature-dependent measurements were repeated using a buffer with lower OG concentration. Figure 6A shows spectra obtained from a sample prepared in buffer with 0.54% OG and heated from 283 to 300 K in nine steps. Spectra taken at higher temperatures correspond to decreased absorption at 873 nm. As shown, heating of this sample led for a large part to the dissociation of the B873 complex into B777 with only small amounts of B820 present at intermediate temperatures. Figure 6B shows data obtained from the same sample recooled to 286 K, further to 284 K and further down to 282 K. Storage overnight at 277 K led to formation of the B873 complex again (not shown). In analogy to the experiments using samples containing 0.8% OG, spectra of the sample measured upon recooling did clearly not resemble the spectra obtained during the heating trajectory. In the first cooling step, the B820 spectrum appeared. Further cooling showed intermediate spectra similar to the intermediate spectra obtained in the temperature-dependent B820−B873 reassociation experiments, using 0.8% OG, and similar to spectra obtained in the detergent-variation experiment. Figure 7 shows the difference spectra of the spectra in Figure 6: each spectrum is the difference of two successive spectra measured during the heating process. The absorption spectra obtained at different temperatures show that the B873 peak did not only disappear upon heating but that the peak maximum also blue-shifted by about 3 nm. The successive difference spectra upon heating show a more drastic blue shift: the peak of the temperature-induced bleaching shifted from 877 to 866 nm (Figure 7A). This shift was not observed for heating of samples with 0.8% OG, where all the difference spectra of spectra at increased temperatures had a negative peak at 873 nm and a positive peak at 820 nm (not shown). Because the intermediate spectra that we observed upon reassociation might indicate that the protein was still slowly equilibrating, we thermostated samples at one fixed temperature for 24 h. Within this period, we did not observe any slow spectral changes except a peak appearing around 777 nm and a slow decrease of the other peaks. The peak at 777 nm did not disappear after storage of the sample at 4 °C overnight and, hence, could be ascribed to the occurrence of free pigments, showing degradation of the proteins. Therefore, we did not perform measurements over longer time intervals.

We tried to induce the B873−B820 transition by varying the protein concentration. For this experiment, the temperature or detergent concentration was adjusted so that the absorption spectrum of the sample contained both the B820 peak and the B873 peak. From this starting point halfway through the transition, the concentration of protein was increased or decreased to direct the transition toward

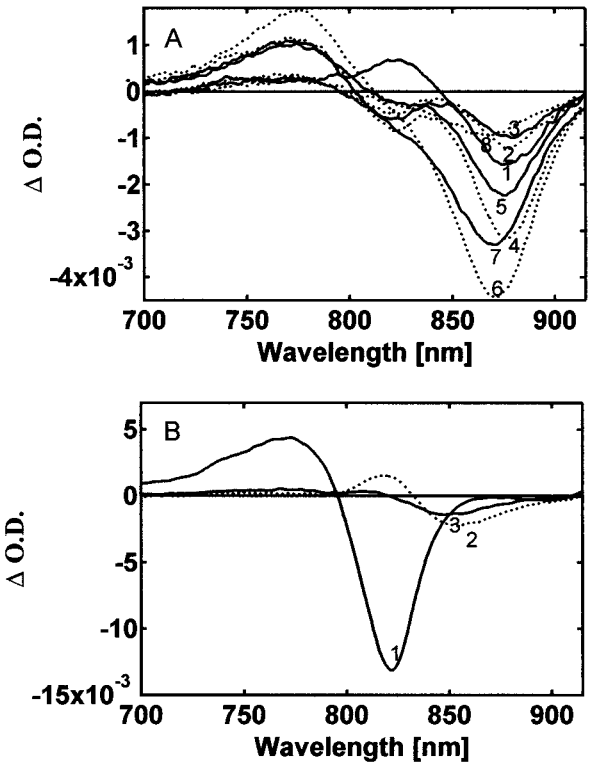

FIGURE 7: Difference spectra of the absorption spectra in Figure 7, obtained by taking the difference of two successive spectra measured during the heating process (A) and during the recooling process (B). In panel A, numbers belong to the following temperature differences, respectively (alternating straight lines and dotted lines): (1) 286−283 K, (2) 288−286 K, (3) 290−288 K, (4) 295−290 K, (5) 296−295 K, (6) 299−296 K, (7) 301−299 K, (8) 302−301 K. In panel B numbers belong to the following temperature differences: (1) 302−286 K, (2) 286−284 K, and (3) 284−282 K.

formation of B873 or dissociation into B820, respectively. However, changing the protein concentration by 3 orders of magnitude did not change the shape of the spectra. In contrast to this, from this starting point halfway through the transition, small changes in the detergent concentration (0.005%) or temperature (1 °C) did alter the spectrum. This finding suggests that the transition is modulated by the CMC of the detergents, rather than by the protein concentration.

We wanted to compare the thermodynamic parameters needed for the B820−B873 reaction with the thermodynamic parameters needed for the B777−B820 reaction, although we are aware that interpretation of these parameters is hampered by uncertainty of the detergent interaction. Hereto, the free enthalpy and entropy needed for the B873−B820 dissociation was calculated from the temperature-dependent dissociation spectra obtained from samples containing 0.8% OG, showing a two-state dissociation reaction. To calculate the constants for association, it was assumed that the B873 complexes consisted of the 16 B820 subunits and that the temperature-dependent dissociation of B873 into B820s was a two-state reaction. This appraoch was supported by the fact that no spectral intermediates appeared and only one isosbestic point was observed. Figure 8 shows a Hill plot of the linear logarithm of the association constants plotted versus the reciprocal temperature. The thus obtained changes in free enthalpy and free entropy associated with the B820−B873 association (0.8% OG) were $\Delta H° = -2391$ (446) kJ mol^{-1} and $\Delta S° = -6.3$ (1.6) kJ mol^{-1} K^{-1}. The values for the thermodynamic parameters are that large, because the full association of B820 into B873 is considered here as one step, including a 16-fold oligomerization (see Discussion, section 3.2.1).

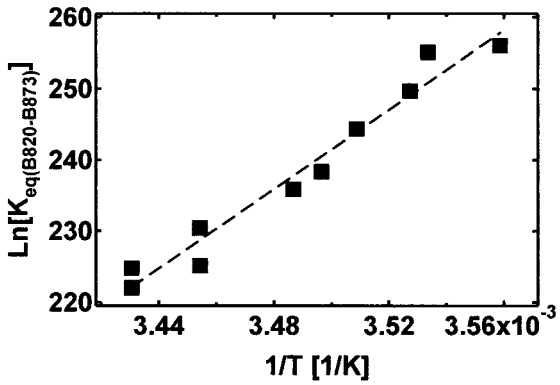

FIGURE 8: Hill plot for the B820−B873 association: The logarithm of the association constants for the association of B820 into B873 are plotted versus reciprocal temperature. The change in enthalpy $\Delta H°$ is −2391(446) kJ mol^{-1} and the change in free entropy is $\Delta S°$ is −6.3(1.6) kJ mol^{-1}K^{-1}. To obtain the association constants, a series of absorption spectra with inreased temperature was fitted with a linear combination of a B873 and a B820 spectrum to estimate the concentration of each species. Assuming a 16-fold association reaction, the association constants were calculated from $K_a = [B873]/[B820]^{16}$.

We performed a control experiment using samples containing free BChl *a*, diluted from a stock solution in methanol into a buffer containing 0.8% OG (final concentration methanol less than 1 vol %). Samples were treated similar to LH1 samples on which temperature measurements were performed: they were stored at 4 °C overnight, heated to 298 K and recooled successively to 278 K. No spectral changes were observed now, demonstrating that the intermediate spectral form, observed in LH1 samples during the B820−B873 transition, originates from the protein−pigment complexes and not from aggregation of free pigment molecules.

2.3. Spectral Three-Component Fitting. Both the series of detergent-dependent spectra, shown in Figure 3, and temperature-dependent spectra of recooled samples, shown in Figure 5B, were fitted using a global analysis three-component spectral fitting procedure. Two components were fixed to the measured B820 and B873 spectra. The third component was fitted as a sum of two skewed gaussians with both variable widths and amplitudes. The use of two gaussians instead of one allowed the fitted spectrum to possess a blue tail similar to the experimental B820 and B873 spectrum and resulting from vibrational modes and/or high energy excitonic components. Neither the detergent-dependent series nor the temperature-dependent series of spectra, in which samples were recooled after heating could be fitted with only a linear combination of a B820 spectrum and a B873 spectrum. Note that in contrast to this, spectra measured of samples that were heated (showing dissociation of B873 into B820, Figure 5A) could be fitted with this combination. The results were used to calculate the contribution of free enthalpy and entropy for the oligomerization of B820 into B873 (see above, section 2.2). Figure 9A shows the spectra resulting from fitting of the detergent-dependent transition spectra. Figure 9B shows the fractional contributions of the

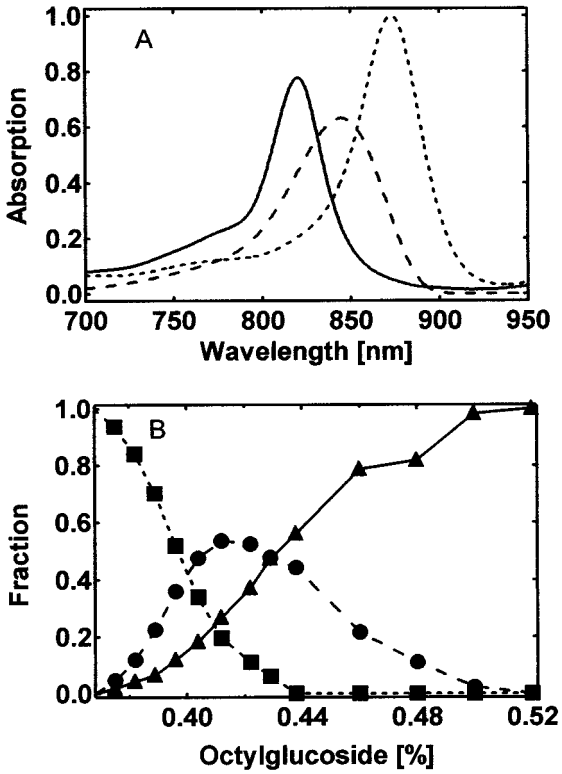

FIGURE 9: A global analysis three-component fit of the series of detergent-dependent absorption spectra. All spectra of the series were fitted with three spectral components, of which two were fixed as the measured B820 and B873 spectrum and of which the third was fitted with two Gaussians with variable widths and amplitudes. (A) The fit-spectra (straight line is the B820 spectrum, dotted line is the B873 spectrum and dashed line is the fitted intermediate spectrum). (B) The relative contributions of each spectrum as a function of the detergent concentration (squares give the B873 fraction, triangles the B820 fraction and circles the intermediate fraction).

three spectral components as a function of the detergent concentration. Note that the sum of the fractions of the three components was close to 1. For both the detergent-dependent spectra and the temperature-dependent spectra all fitted spectra reflecting the intermediate had absorption maxima located around 850 nm (varying from 845 to 853 nm). The full-width half-maximum (fwhm) of the fitted intermediate spectra varied from 880 to 1050 cm^{-1}, which was in all cases broader than the fwhm of the B820 and B873 spectra (540 and 570 cm^{-1}, respectively). The total area of the fitted intermediate spectra was similar to the total area of the B820 and B873 spectra, with the maximal fractional contribution of the intermediate component varying from 0.4 to 0.7. We tried to fit a series of temperature-induced transition spectra using the fitted intermediate spectrum of a global analysis fit on the detergents-induced series. This only yielded good-quality fits if the width and skewness of the intermediate fit-spectrum was allowed to vary in the fitting procedure.

Summarizing, the shape (width and skewness) and the maximal fractional contribution of the intermediate fitted spectrum varied for different experiments and for fitting of temperature- and detergents-induced transition spectra, but the peak maximum was always located around 850 nm. Although only one intermediate-fitting component was needed for good-quality fits, the broad width of the fit spectrum relative to the B820 and B873 spectrum could indicate that the spectrum arises from a linear combination of several intermediate components.

3. DISCUSSION

3.1. Oligomerization of B777 into B820. We report here that the association of B777 into B820 is a dimeric association reaction. This result agrees with spectroscopic evidence that the B820 subunit has to be dimeric (*20*, *21*) and with the conclusions of Loach and Parkes-Loach (*19*). Most likely, the B820 subunits are therefore the dimeric units, of which 16 oligomerize to form a B873 ring (*8*). In contrast to our results, Sturgis and Robert reported a tetramerization (*15*). A difference in our experiments compared to theirs is the range of the total polypeptide concentration. We have induced association by increasing the total concentration a 1000-fold in the nano- to micromolar range, whereas in the experiments of Sturgis and Robert the concentration was only increased 10-fold, in the millimolar range. Also, we probably used a lower detergent concentration; however, our concentration of 0.8% should be above the CMC at room temperature, similar as in their experiments. Perhaps it is possible that the type of association depends on the peptide concentration (together with the detergent concentration) in such a way that at high detergent and peptide concentrations B820 dimers will immediately dimerize to form tetramers, but without further shifting of the absorption. For the thermodynamic parameters $\Delta H°$ and $\Delta S°$, associated with the B820 association, we found values in the same range as found by Sturgis and Robert, although we used association constants that were calculated assuming a dimeric reaction, instead of a tetramerization.

We will speculate which factors might attribute to the change in free energy upon association and to which extent. Factors that possibly contribute to the change in enthalpy upon association of the B777 monomers into the B820 subunit are the formation of two hydrogen bonds (probably cross binding from the α-polypeptide BChl keto $C13^1$ to the Tyr4 and/or Trp6 of the *β*-polypeptide and from the Ser5 and/or Thr6 of the α-polypeptide to the *β*-polypeptide BChl keto $C13^1$), of one ion pair (*15*, *19*) and of a BChl-BChl dimer. The first two factors could contribute to maximally about 50 kJ mol^{-1} and the latter to about 40 kJ mol^{-1} (*23*). Furthermore, greater backbone stabilization is measured for polypeptides in the B820 subunit than in the B777 monomer (*31*) and intra-polypeptide hydrogen bonds might be formed upon association, giving an energetic contribution of about 20 kJ mol^{-1}/bond (*36*). Counting all known enthalpic contributions, assuming that each polypeptide of a formed heterodimer is stabilized by one intra-hydrogen bond, this yields $40 + 50 + 20 + 20$ kJ $mol^{-1} = 130$ kJ mol^{-1} for the total change in enthalpy upon dimer formation. This number is less than the total enthalpy change that we measured, but can explain a major part of it. Efficient packing of the polypeptides upon dimerization might contribute as well glycine residues, of which one is present in the transmembrane region of both the α-and *β*-polypeptides of *Rs. rubrum*, can be involved in dimerization of transmembrane peptides (*37*) and mediate helix−helix interactions by efficient packing (*38*). Factors that contribute to the change in entropy are restriction of both the polypeptide side-chain motion and backbone stabilization upon association, partly compensated by the decrease of solvent accessibility (*31*).

3.2. Oligomerization of B820 into B873. 3.2.1. Thermodynamics of the B820−B873 Transition. To understand the oligomerization of B820 into B873, the thermodynamics of the detergent in the solvent has to be taken into account. In contrast to the B777−B820 oligomerization process, the B820−B873 oligomerization process seems to be coupled with a phase transition of the OG molecules. As mentioned in the introductory portion of this paper, it is unclear at which concentration OG reaches its CMC. The CMC of the detergent we used is estimated to be in the range of 0.44−0.68% (Calbiochem, San Diego, CA). However Paula et al. estimated this to be between 0.6 and 0.8% depending on the temperature (*33*). In both cases, a temperature-mediated dissociation or association reaction might be coupled with a phase transition of the detergent. Considering a CMC in the range of 0.4−0.6%, our two types of sample preparations containing 0.54 and 0.8% OG should contain OG concentrations on the onset and well-above the CMC, respectively. However, if the CMC is in the range of 0.6−0.8%, the first experiment will represent a dissociation reaction performed below the CMC. In that case, the transition in the latter experiment using 0.8% OG might be mediated by a phase transition of the detergent: according to Paula et al., the CMC has a value of 27.9 mM (0.81%) at $T = 286$ K and a value of 22.6 mM (0.66%) at $T = 300$ K (*33*). This would mean that in our temperature-induced transition experiments in which we used a detergent concentration of 0.8%, the detergent concentration was right at the onset of the CMC at 286 K and above the CMC at 300 K. We observed that heating from 282 to 300 K led to dissociation of the B873 complex starting at $T = 286$ K and accomplished at 300 K. Referring to the same studies of Paula et al., no phase transition is expected in our temperature-mediated experiments using 0.54% OG for temperatures up to at least 300 K [at $T = 313$ K, the CMC was measured to be 20.8 mM, 0.61%, and at higher temperatures the CMC increases again (*33*)]. Here we observed a rapid collapse of the B873 peak already at temperatures above 290 K. The appearance of monomeric B777 together with a decreasing and blue-shifting B873 peak could be explained by an opening of the LH1 ring via the loss of some dissociated subunits, giving a combination of incomplete (blue-shifted) rings and monomeric polypeptides as reaction products. In the studies of Miller et al. (*13*), it was found that reassociation of B873 from B820 subunits yielded an absorption spectrum that was slightly blue-shifted from the original B873 spectrum; this could be the same phenomenon having uncompleted rings, appearing in the reassociation process.

The changes in free enthalpy and entropy for the oligomerization of B820 subunits into B873 show values that are approximately 12-fold of the values for changes in free enthalpy and entropy associated with a dimerization of B777 into B820 subunits. Although these numbers must be viewed with some caution, this suggests that the intersubunit forces between the α and β polypeptides in the dimer are of the same order of magnitude as the intrasubunit forces between the subunits in the LH1 ring. Factors that could contribute to the change in enthalpy are, first, a change of hydrogen bonding of the Trp11 residue of the α-polypeptide and the Trp9 of the β-polypeptide to the C3[1]carbonyl group. Second, two ion pairs might be formed per B820 unit, so 32 pairs in total, giving a maximal contribution of about 200 kJ mol^{-1}. Further, changes of water structures around the protein will add to the change in free enthalpy and free entropy, assuming that the oligomerization reaction is driven by hydrophobic forces. If the B820−B873 association reaction involves a phase transition of the detergent, breaking or formation of detergent micelles probably contributes to the total change in free energy involved [the change in free energy for breaking OG micelles is 18−19 kJ/mol detergents (*33*)]. Going from below to above the micellar phase in the association reaction, detergent molecules will either micellize of associate with the protein complexes, in both cases giving a positive contribution to the change in free enthalpy. Thus, the actually change in free enthalpy contributing from dissociation of the protein complex might be smaller than the value we found.

3.2.2. Origin of Spectral Intermediates: Comparison with Simulated Absorption Spectra. For better understanding of the origin of the spectral intermediates that we observe, we compared our spectra with simulated absorption spectra of a set of aggregates, consisting of parts ("arcs") of an LH1 ring that varied in aggregation size. This approach conforms to the study of Westerhuis et al., who used simulated spectra of a set size-ranged aggregates for comparison with a series of detergent-isolated LH1 complexes of *Rb. sphaeroides* (*39*). For our simulations, the pigment geometry within a heterodimeric unit was adapted from the structure of the LH2 complex of *Rs. acidophila*, which has a C_9 symmetry (*40*). Also the interdimer distance was adapted from the structure and the ring size expanded to fit 16 heterodimers. This template was used as a model for the simulation of the LH1 ring. The structural parameters in this model are comparable with the parameters used in the model of Hu and Schulten, who modeled computanionally the LH1 complex of *Rb. sphaeroides* (*41*), with the small difference that they used the heterodimer structure from LH2 of *Rs. Molischianum* as a template [the B850 pigments in LH2 of *Rs. Molischianum* have a nearest-neighbor distance of 9.4 Å and a dipole−dipole coupling of 339 cm^{-1} whereas the B850 pigments in LH2 of *Rs. acidophila* have nearest-neighbor distance of 9.5 Å and a dipole−dipole coupling of 322 cm^{-1} (*4*)]. The total blue shift between the absorption maximum of a complete ring of 16 dimers and a dimer was set to 53 nm (the observed blue shift between B873 and B820) by adjusting the intradimer coupling to 600 cm^{-1}. Note that in reality, a significant part of the shift between the B820 and B873 absorption could also be caused by mixing of the charge-transfer states with the excitonic states of closely interacting pigments (*42*−*45*); this causes the strong Stark signal of LH1 that is absent in B820 (*46*). The inhomogeneous line width was set to 600 cm^{-1}. Simulations of absorption spectra were performed according to Wendling et al. (to be published). Figure 10 shows the simulated spectra of a dimer, 2-fold dimer, 3-fold dimer, 8-fold dimer, and complete ring. In these simulations, going from a full ring to an 8-fold dimer cluster results in the appearance of an absorption peak with a maximum around 864 nm. This is close to the maximal blue shift of the difference spectra shown in Figure 7 (results of heating a sample containing 0.5% OG). The same set of simulations show that only the absorption spectrum of a 2-fold dimer has a maximum close to the maxima of the spectra estimated from global-analysis fitting of our measured transition spectra. The spectrum of a 2-fold dimer has an

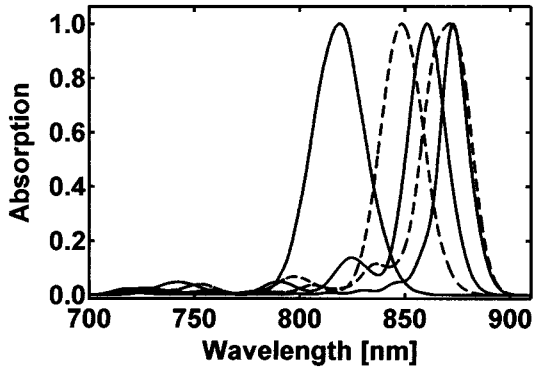

FIGURE 10: Calculated absorption spectra for arc-shaped aggregates consisting of (from left to right): B820, $(B820)_2$, $(B820)_3$, $(B820)_8$, and B873 (full LH1 ring), respectively. For the calculations, the pigment geometry within a heterodimeric unit and the interdimer distance was adapted from the structure of the LH2 complex of *Rs. acidophila*, which has a C9 symmetry, and the ring size expanded to fit 16 heterodimers. The total blue shift between the absorption maximum of a complete ring of 16 dimers and a dimer was set to 53 nm (the observed blue shift between B873 and B820) by adjusting the intradimer coupling to 600 cm^{-1}.

absorption maximum at 848 nm, whereas the maximum of a 3-fold dimer is already much further red shifted (861 nm).

Our observations of an intermediate absorbing around 850 nm match with the observations of Ghosh et al. who noticed that for the reassociation from B777 to B873 "discrete transitory states" appear at 820−825 and 850 nm (*14*) (the 820 nm absorbing form is by now well-known as the B820 subunit). Also Loach et al. mention that when the LH1 of *Rs. rubrum* is converted to B820 subunits by titration with OG, a set of isosbestic points is observed so that only two species are in equilibrium initially and at the end of the titration, but that an intermediate may be present between (*19*). They observed a fast (within seconds) red shift of 820 nm toward 860 nm upon reassociation, followed by a slow final 12−15 nm shift, taking hours to days. Further, Miller et al. measured spectra slightly blue-shifted from the B873 spectrum in the reassociation process (*13*). The forms absorbing around 860 nm are probably the intermediate spectra that we also observed. However, we did not detect any slow equilibration of the protein between the B820 and B873 form for these cases. It is possible that slow equilibration exists, but on a time scale longer than the time in which degradation of the protein takes place. In the above referred Stark experiment, intermediates in the reassociation process were reported that were about 10 nm blue-shifted from B873 and had a large Stark effect (*46*). A spectral form blue shifted from 873 nm was also observed in a stopped-flow experiment, in which B820 in OG was rapidly diluted to induce reassociation, resulting in a spectrum with a maximum around 865 nm (*32*). The kinetics of this reassociation could be reasonably well described by a dimerization of the B820 units, but the residual spectra after fitting of a dimeric reaction fit did display some structure that was maximal around 850 nm. In a reassociation study of the B820 subunit of the LH1 of *Rb. sphaeroides* solubilized in the detergent *n*-octyl-rac-2,3-dipropylsulfoxide (ODPS), an intermediate spectrum was observed with a maximum located at 845 nm (*47*). This spectral form was attributed to the formation of dimers of BChl *a*. Revisiting these results combined with our findings, it is possible that upon the stopped-flow mixing intermediates absorbing around 850 nm were formed together with more complete or full complexes with a more red-shifted absorption. The kinetic stopped-flow results could best be described by a dimerization reaction, also supporting the idea that intermediates exist that are dimers of B820 subunits.

3.2.3. Distribution of Aggregates According to Two Model Association Schemes. Proposing that the association of B820 subunits toward a ring aggregate is a multiple-state reaction, we raised the question whether intermediate aggregates could exist in equilibrium following a cooperative association reaction scheme. In particular, the last step toward formation of a ring aggregate might be highly cooperative (or, turning it around, breaking the ring might cost extra energy compared with further dissociation). Hereto, we calculated the distribution of aggregates at different temperatures according to two possible models of association schemes. In the first scheme, B873 is formed from B820 subunits in four dimerization steps:

Scheme 1

$$16B820 \rightleftharpoons 8(B820)_2 \rightleftharpoons 4(B820)_4 \rightleftharpoons 2(B820)_8 \rightleftharpoons B873 \quad (1)$$

In the second scheme, B873 is formed from B820 subunits in 15 steps:

Scheme 2

$$16B820 \rightleftharpoons 14B820 + (B820)_2 \rightleftharpoons 13B820 + (B820)_3 \rightleftharpoons ... \rightleftharpoons B820 + (B820)_{15} \rightleftharpoons B873 \quad (2)$$

These two schemes were chosen as they represent the two most extreme cases how oligomerization of B820 may occur; a variation of other schemes is conceivable in which association of B820 subunits is combined with clustering of larger aggregates. In our calculations, the total change in free enthalpy and entropy were fixed to be $\Delta H^\circ = -2391$ (446) kJ mol^{-1} and $\Delta S^\circ = -6.3$ (1.6) kJ mol^{-1} K^{-1}; the values that we calculated for the B820−B873 transition (in the presence of 0.8% OG). The total concentration was fixed to be 0.3 μM of "dimer units", which conformed to the concentration we used in the latter experiment. The association reactions where either considered noncooperative, each step having the same association constant (hence, same activation energy), or cooperative by using a set of association constants: K_a for the first association step, ωK_a for the second step, $\omega^2 K_a$ for the third step, etc., toward complete formation of B873. Furthermore, we performed a calculation in which all reaction steps (using either Scheme 1 or Scheme 2) had equal association constants, except the last step toward formation of B873, of which the association constant was set at 10-fold higher. The latter approach would be representative for an association reaction in which breaking the full LH1 ring (the reverse of the last step in the association reaction) would cost extra energy. For several temperatures in the range 277−305 K and for several values of ω the fractional distributions of (B820)-aggregates in equilibrium were calculated. Using Scheme 1, the reaction appears as a two-state reaction, in both the cooperative and noncooperative case. Figure 11 shows the distributions of the dimer units over the set of aggregates, according to Scheme 1 and plotted

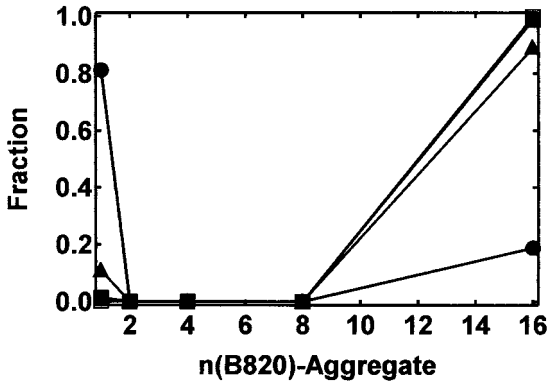

FIGURE 11: Distribution of B820-aggregates in equilibrium, using a model reaction scheme for the B820−B873 transition that includes four dimerization steps (Scheme 1). The fractional contribution of each aggregate $(B820)_n$ is plotted versus the oligomerization number *n*. Symbols represent calculations for $T = 277$ K (open squares), 285 K (filled squares), 295 K (triangles) and 305 K (circles) (results for $T = 277$ K and $T = 285$ K completely overlap).

for different temperatures. The *y*-axis represents the fraction of the total concentration of dimer units while the numbers on the *x*-axis conform to the aggregation state [e.g., 1 is a dimer (or B820), 2 a tetramer ($(B820)_2$), etc.]. The figure shows the (indistinguishable) result for both a noncooperative reaction ($\omega = 1$) and a cooperative reaction ($\omega > 1$). Increasing the temperature induces dissociation of B873 into B820 without fractional contribution of the other aggregates, meaning that the reaction appears as a two-state reaction without the occurrence of intermediates in equilibrium. Using Scheme 2, the reaction appeares as a two-state reaction in case of high cooperativity (Figure 12A) but results in a more flat distribution of aggregates at transition temperatures in case of low or no cooperativity (Figure 12, panels B and C). Increasing the association constant for the last step toward B873 formation (Figure 12D) does increase the occurrence of B873 at lower temperatures and thereby changes the distribution from flat toward a two-state reaction distribution. Summarizing, an equilibrium in which intermediates coexist together with B820 or B873 was only obtained by a step-by-step association scheme (Scheme 2) if no or only low cooperativity was introduced. An equilibrium in which only B820 and B873 are present was obtained in using Scheme 1 for all cases (no, low or high cooperativity) and by introducing high cooperativity in Scheme 2. The occurrence of intermediates in equilibrium is reduced by introducing extra cooperativity for the last step only, compensated by the occurrence of more B873.

An interesting result of our modeling is that where intermediates appear, there is a high abundance of aggregates that approach B820 or B873 (like tetramers or 15-fold aggregates) and the relative absence of intermediate-sized aggregates. An exception is the case of no cooperativity in a step-by-step association reaction (Figure 12C), where all intermediates have the almost the same occurrence. The latter case seems unrealistic because B820 and B873 form only a small contribution of the total number of aggregates, contradictonary to experimental results in which the absorption spectrum is dominated by B820 or B873. The occurrence of both small and very large aggregates, however, would match with our experimental observations if we presume there that

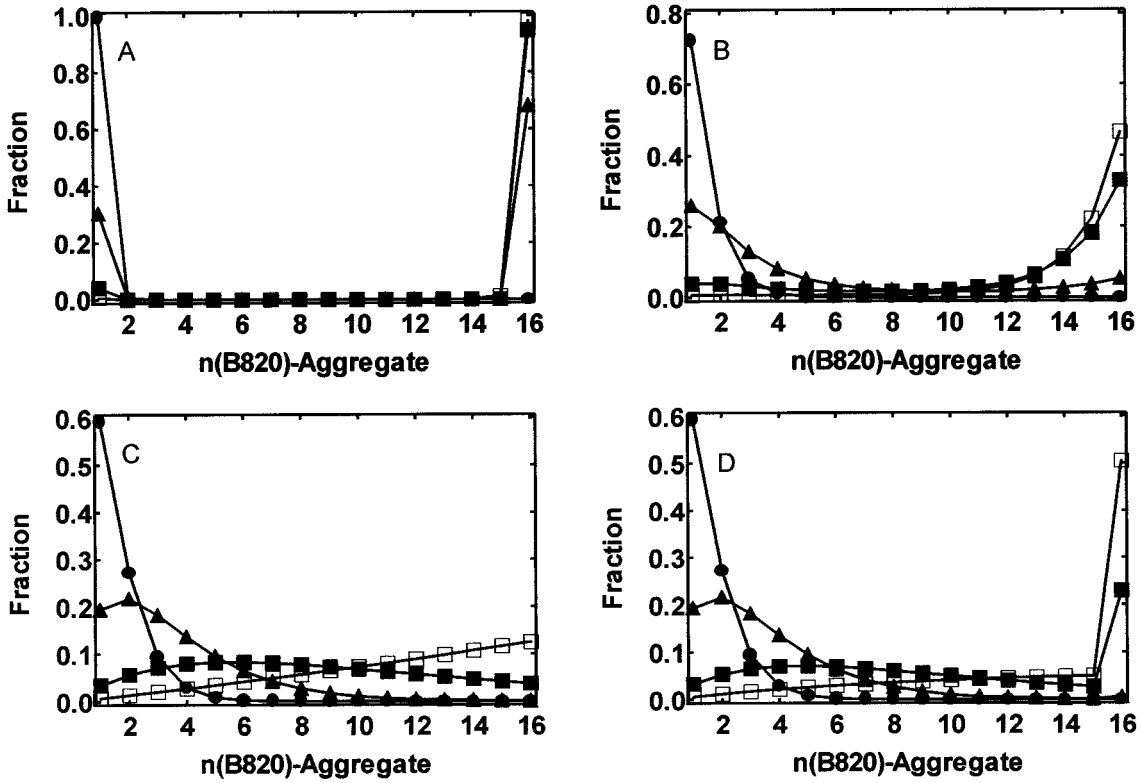

FIGURE 12: Distribution of B820-aggregates in equilibrium, using a model reaction scheme for the B820−B873 transition that includes fifteen dimerization steps (Scheme 2). The fractional contribution of each aggregate $(B820)_n$ is plotted versus the oligomerization number *n*. Symbols represent calculations for $T = 277$ K (open squares), 285 K (filled squares), 295 K (triangles) and 305 K (circles). Distributions were calculated using a cooperativety constant $\omega = 2$ (A), $\omega = 1.05$ (B), or $\omega = 1$ (C) (no cooperativity), respectively, or using $\omega = 1$ but using a 10-fold higher association constant for the last step toward formation of B873 than for the other steps (D), suggesting extra stability of a closed LH1 ring.

the component absorbing at 850 nm is tetrameric and that spectra, which are blue-shifted a few nanometers from B873, represent large but incomplete rings. It is also demonstrated with our models that a highly cooperative reaction will lead to a transition in which only B820 units and B873 occur, resembling our heating experiments. However, the observed hysteresis effect cannot be explained by our model reaction schemes. Probably formation or breaking of the detergent molecules should be taken into acount in a reaction model to simulate the hysteresis. Still, using our models, we can speculate about the possible types of transitions. Using Scheme 2, a completely noncooperative reaction appears unrealistic. But introducing an extra barrier for breaking of the LH1 ring in a further noncooperative reaction could describe our observations of an intermediate spectral form, being a small aggregate of B820. In case the LH1 complex would consist of unclosed rings, as proposed by Jungas et al. (*11*), a moderative cooperative step-by-step association reaction is needed to obtain an equilibrium in which very small and large aggregates exist [changing the stoichiometry from 16 to 12, as also proposed by Jungas et al., did not significantly change the results (not shown)].

Results using the second model scheme demonstrate that it is possible to have equilibrium states in which a number of different-sized oligomers exist. Thus, our observations of intermediate spectral forms do not necessarily imply that the protein was still slowly equilibrating between the B820 and B873 form.

SUMMARY

We have evidence that the transition of B820 to B873 includes (at least) one intermediate conformation consisting of a spectral form absorbing around 850 nm. The set of absorption spectra of the B820−B873 transition during reassociation did not have an isosbestic point and could not be fitted with a linear combination of a B820 and a B873 spectrum. The small blue shift of the B873 peaks of Figure 6 suggest that more intermediate forms can be formed, depending on the precise detergent conditions.

The hysteresis effect of our temperature measurements suggests either a high transition barrier between the full B873 form and the intermediate B850 form compared to the transition barrier between the B850 and the B820 state or a different pathway for reassociation than for dissociation. Both cases could explain how the protein can be trapped in the intermediate B850 state during reassociation, whereas in the reversible dissociation no intermediates are observed.

ACKNOWLEDGMENT

Markus Wendling is gratefully acknowledged for providing simulations of absorption spectra of a series of size-ranged antenna aggregates.

REFERENCES

1. Drews, G. (1985) *Microbiol. Rev. 49*, 59−70.
2. van Grondelle, R., Dekker, J. P., Gillbro, T., and Sundström, V. (1994) *Biochim. Biophys. Acta 1187*, 1−65.
3. Fleming, G. R., and van Grondelle, R. (1994) *Phys. Today 47*, 48−55.
4. Sundström, V., Pullerits, T., and van Grondelle, R. (1999) *J. Phys. Chem. B 103*, 2327−2346.
5. Brunisholz, R. A., and Zuber, H. (1988) in *Photosynthetic light-harvesting systems* (Scheer, H., and Schneider, S., Eds.) pp 103−114, de Gruyter, New York.
6. McDermott, G., Prince, S. M., Freer, A. A., Hawthornthwaite-Lawless, A. M., Papiz, M. Z., Cogdell, R. J., and Isaacs, N. W. (1995) *Nature 374*, 517−521.
7. Koepke, J., Hu, X., Muenke, C., Schulten, K., and Michel, H. (1996) *Structure 4*, 581−597.
8. Karrasch, S., Bullough, P. A., and Ghosh, R. (1995) *EMBO J. 14*, 631−638.
9. Francia, F., Wang, J., Venturoli, G., and Melandri. B. A., Barz, W. P., and Oesterhelt, D. (1999) *Biochemistry 38*, 6834−6845.
10. Frese, R. N., Olsen, J. D., Branvall, R., Westerhuis, W. H. J., Hunter, C. N., and van Grondelle, R. (2000) *Proc. Natl. Acad. Sci. U.S.A. 97*, 5197−5202.
11. Jungas, C., Ranck, J.-L., Rigaud, J.-L., Joliot, P., and Verméglio, A. (1999) *EMBO J. 18*, 534−542.
12. Loach, P. A., Parkes-Loach, P. S., Miller, J. F., Hichigeri, S., and Callahan, P. M. (1985) in *Molecular Biology of the Photosynthetic Apparatus* (Arntzen, C., Bogorad, L., Bonitz, S., and Steinback, K., Eds.) pp 197−209, Cold Spring Harbor Symposium, Plainview, NY.
13. Miller, J. F., Hinchigeri, S. B., Parkes-Loach, P. S., Callahan, P. M., Sprinkle, J. R., Riccobono, J. R., and Loach, P. A. (1987) *Biochemistry 26*, 5055−5062.
14. Ghosh, R., Hauser, H., and Bachofen, R. (1988) *Biochemistry 27*, 1004−1014.
15. Sturgis, J., and Robert, B. (1994) *J. Mol. Biol. 238*, 445−454.
16. Bustamante, P. L., and Loach, P. A. (1994) *Biochemistry 33*, 13329−13339.
17. Davis, C. M., Parkes-Loach, P. S., Cook, C. K., Meadow, K. A., Bandilla, M., Scheer, H., and Loach, P. A. (1996) *Biochemistry 35*, 3072−3084.
18. Parkes-Loach, P. S., Sprinkle, H. J. R., and Loach, P. A. (1988) *Biochemistry 27*, 2718−2727.
19. Loach, P. A., and Parkes-Loach, P. S. (1995) in *Anoxygenic Photosynthetic Bacteria* (Blankenschip, R. E., Madigan, M. T., and Bauer, C. D., Eds.) Chapter 21, pp 437−471, Kluwer Academic Publishers, Dordrecht, The Netherlands.
20. van Mourik, F., van der Oord, C. J. R., Visscher, K. J., Parkes-Loach, P. S., Loach, P. A., Visschers, R. W., and van Grondelle, R. (1991) *Biochim. Biophys. Acta 1059*, 111−119.
21. Visschers, R. W., Chang, M. C., van Mourik, F., Parkes-Loach, P. S., Heller, B. A., Loach, P. A., and van Grondelle, R. (1991) *Biochemistry 30*, 2951−2960.
22. Visschers, R. W., van Mourik, F., Monshouwer, R. and van Grondelle, R. (1993) *Biochim. Biophys. Acta 1141*, 238−244.
23. Scherz, A., and Rosenbach-Belkin, V. (1988) *Proc. Natl. Acad. Sci. U.S.A. 86*, 1505−1509.
24. Robert, B., and Lutz, M. (1985) *Biochim. Biophys. Acta 807*, 10−23.
25. Cotton, T. M. (1976) Ph.D. Thesis, Northwestern University, Evaston, IL.
26. Olsen, J. D., Sturgis, J. N., Westerhuis, W. H. J., Fowler, G. J. S., Hunter, C. N., and Robert, B. (1997) *Biochemistry 36*, 12625−12632.
27. Davis, Ch. M., Bustamante, P. L., Todd, J. B., Parkes-Loach, P. S., McGlynn, P., Olsen, J. D., McMaster, L., Hunter, C. N., and Loach, P. A. (1997) *Biochemistry 36*, 3672−3679.
28. Parkes-Loach, P. S., Michalski, T. J., Bass, W. J., Smith, U., and Loach, P. A. (1989) *Biochemistry 29*, 2951−2960.
29. Sturgis, J. N., Olsen, J. D., Robert, B., and Hunter, C. N. (1997) *Biochemistry 36*, 2772−2778.
30. Fowler, G. J. S., Visschers, R. W., Grief, G. G., van Grondelle, R., and Hunter, C. N. (1992) *Nature 355*, 848−850.
31. Sturgis, J., Robert, B., and Goormagtigh, E. (1998) *Biophys. J. 74*, 988−994.
32. van Mourik, F., Corten, E. P. M., van Stokkum, I. H. M., Visschers, R. W., Loach, P. A., Kraayenhof, R., and van Grondelle, R. (1992) in *Research in Photosynthesis* (Murata, N., Ed.) pp 101−104, Kluwer Academic Publishers, The Netherlands.

33. Paula, S., Sus, W., Tuchtenhagen, J., and Blume, A. (1995) *J. Phys. Chem. 99*, 11742−11751.
34. Weigl, J. W. (1953) *J. Am. Chem. Soc. 75*, 999−1000.
35. van Stokkum, I. H. M., Linsdell, H., Hadden, J. M., Haris, P. I., Chapman, D., and Bloemendal, M. (1995) *Biochemistry 34*, 10508−10518.
36. Lantz, M. A., Jarvis, S. P., Tokumoto, H., Martynski, T., Kusumi, T., Nakamura, C., and Miyake, J. (1999) *Chem. Phys. Lett. 315*, 61−68.
37. Lemmon, M. A., Treutlein, H. R., Adams, P. D., Bruenger, A. T., and Engelman, D. M. (1994) *Nat. Struct. Biol. 1*, 157−163.
38. Javadpour, M. M., Eilers, M., Groesbeek, M., and Smith, S. O. (1999) *Biophys. J. 77*, 1609−1618.
39. Westerhuis, W. H. J., Hunter, C. N., van Grondelle, R., and Niederman, R. A. (1999) *J. Phys. Chem. B. 103*, 7733−7742.
40. Freer, A., Prince, S., Sauer, K., Papiz, M., Hawthornthwaite-Lawless, A., McDermott, G., Cogdell, R., and Isaacs, N. W. (1996) *Structure 4*, 449−462.
41. Hu, X., and Schulten, K. (1998) *Biophys. J. 75*, 683−694.
42. van Mourik, F., Visschers, R. W., and van Grondelle, R. (1992) *Chem. Phys. Lett. 195*, 1−7.
43. Monshouwer, R., Abrahamsson, M., van Mourik, F., and van Grondelle, R. (1997) *J. Phys. Chem. B 101*, 7241−7248.
44. Koolhaas, M. H. C., Frese, R. N., Fowler, G. J. S., Bibby, T. S., Georgakopoulou, S., van der Zwan, G., Hunter, C. N., and van Grondelle, R. (1998) *Biochemistry 37*, 4693−4698.
45. Scholes, G. D., and Fleming, G. R. (2000) *J. Phys. Chem. B. 104*, 1854−1868.
46. Beekman, L. M. P., Steffen, M., van Stokkum, I. H. M., Olsen, J. D., Hunter, C. N., Boxer, S. G., and van Grondelle, R. (1997) *J. Phys. Chem. B 101*, 7284−7292.
47. Visschers, R. W., Nunn, R., Calkoen, F., van Mourik, F., Hunter, C. N., Rice, D. W., and van Grondelle, R. (1992) *Biochim. Biophys. Acta 1100*, 259−266.

BI010163F